Low-Pressure Heat Transfer Fluids for Pumped Two-Phase Cooling

Nitin Karwa[1], Samuel Yana Motta[2]
Honeywell International Inc.,
[1]Honeywell India Technology Center, 122018 Gurgaon, India,
Email: Nitin.Karwa@Honeywell.com
[2]20 Peabody Street Buffalo, NY 14210, USA
Email: Samuel.YanaMotta@Honeywell.com

ABSTRACT

The increasing heat flux from chips, and high server- and rack-level heat densities in high performance computing infrastructure have resulted in the advent of advanced cooling technologies, such as cold plates and immersion cooling. Water-based heat transfer fluids are used in cold plate systems. It is widely debated if it will be effective and energy efficient for cooling of chips with heat flux exceeding 500 kW/m^2. Two-phase cooling with dielectric fluorinated fluids, such as hydrofluorocarbons (HFC), hydrochlorofluoroolefins (HCFO), hydrofluoroolefins (HFO), hydrofluoroethers (HFE), in cold plates may be more suited to sustain the ever-increasing heat density. The need to cool devices with ever-increasing power density, the push towards lower global warming potential fluids, and the occupational and equipment safety requirements has motivated a search for suitable two-phase heat transfer fluids. This paper introduces the environmental and occupational safety aspects, and effect of global regulations on the selection of fluorinated heat transfer fluids for use in data centers. This study presents drop-in performance evaluation of low-pressure fluid options, namely, HCFO-1233zd (E), HFC-245fa and HFE-7000, in pumped two-phase cooling system for heat flux up to 640 kW/m^2. Performance is also compared with single-phase water cooling. The performance is reported in terms of thermal resistances of the cold plate and the system. Compared to water cooling, two-phase cooling achieved lower junction temperatures and more uniform cooling at much lower flow rate. System level thermal resistance was lower for two-phase cooling, except with HFE-7000, which had considerably high thermal resistance in the condenser. Unlike HCFO-1233zd(E), HFC-245fa will be eventually phased-down globally, therefore it is not a sustainable long-term option for the industry. This study shows that HCFO-1233zd(E) is a feasible low-pressure heat transfer fluid option for thermal management of high performance computing infrastructure.

KEY WORDS: high performance computing, pumped two-phase cooling, microchannel cold plate, water, low-pressure fluid, refrigerant, HCFO-1233zd(E), HFC-245fa, HFE-7000, thermal resistance, occupational safety, environmental regulations

NOMENCLATURE

A_H	heated area, m^2
Co	confinement number, –
D_H	hydraulic diameter, m
g	acceleration due to gravity (9.81), m/s^2
H	microchannel height, m
I	current, A
k_{CU}	thermal conductivity of copper, W/(m·°C)
L	channel length, m
N	number of channels, -
$\ddot{q}$	heat flux, W/m^2
Q	heat input, W
R	thermal resistance, °C/W
t	thickness of base, m
T	temperature, ºC
V	voltage, V
W	microchannel width, m
W_f	fin width, m

Greek symbols

σ	surface tension, N/m

Subscripts

B	base
C	Condenser
CP	cold plate
J	junction
SYS	system
OUT	outlet
SAT	saturation
W	water

INTRODUCTION

The increasing power levels of microprocessors and the use of racks with heat loads exceeding 30 kW in high performance computing (HPC) applications necessitates direct liquid cooling of the microprocessors in the servers. Liquid cooling is achieved by either submerging the electronics into a pool of heat transfer fluid, also referred as immersion cooling, or attaching a cold plate to the surface of the electronics. Water-based heat transfer fluids are widely used in cold plate systems for single-phase convective cooling of chips with heat flux of 500 kW/m^2 at ASHRAE W4 conditions but it is widely debated if it will be effective and energy efficient with further increase in heat flux. The key limitation of water cooling for very high heat dissipation application is its limited cooling capacity, and the resulting flow rates may not be practical. To enhance the heat transfer coefficient in single-phase flow to meet the thermal performance requirements in the future, very narrow flow passages shall be required, which will increase manufacturing costs, flow maldistribution, fouling and pumping power.

Two-phase cooling using dielectric fluids may be able to overcome these challenges. Fluorinated fluids, such as HFC, HFO, HCFO and HFE, have been investigated as potential heat transfer fluids for electronics cooling. HFC, HCFO and HFO

are widely used as refrigerants in vapor compression systems. Refrigerants with normal boiling point close to room temperature are referred to as low-pressure refrigerants. HFE fluids with normal boiling point in excess of 30 ºC are also used as dielectric heat transfer fluids.

Karwa [1] experimentally evaluated drop-in performance of water and refrigerants HCFO-1233zd(E), HFO-1234ze(E) and HFC-134a in microchannel cold plate for cooling of high heat flux CPU. It was demonstrated that two-phase cooling has a significantly reduced flow rate as compared to water cooling and it can substantially improve the heat transfer coefficient and temperature uniformity as compared to water.

Saums et al. [2] presented a case study on cooling of power electronic devices using single-phase water cooling in aluminum cold plates and two-phase HFC-134a cooling in copper cold plates. For a fixed junction temperature, HFC-134a could remove 40% more heat than water cooling, and the HFC-134a flow rate required in the tests was only 20% of water. The HFC-134a system was more compact than the water-cooled system.

Hannemann et al. [3] compared single-phase water cooling with two-phase R-134a cooling for a 200 W heat load. The coolant temperature rise was 10 °C for the water but negligible for HFC-134a. The HFC-134a system had a mass flow rate, pumping power and a condenser size that were 21%, 10% and 50% of the single-phase water cooling system, respectively.

Olivier et al. [4] evaluated drop-in performance of single-phase water, a 50% water–ethylene glycol mixture and several two-phase heat transfer fluids using a semi-empirical model for a microchannel cold plate. The microchannel copper cold plate had a footprint 20 mm × 20 mm and the channel height, width and spacing were 1.7 mm, 0.17 mm and 0.17 mm, respectively. The heat fluxes were varied between 200 and 1500 kW/m^2 and mass fluxes between 300 and 1000 kg/m^2·s for two-phase flow and 300–6000 kg/m^2·s for single-phase flow. They reported that HFC-134a has the lowest junction temperature, followed by HFO-1234yf and HFO-1234ze. The average junction temperature for HFC-134a two-phase cooling was 9 to 15 °C lower than for single-phase water cooling. For water cooling to match the junction temperature uniformity of HFC-134a, the flow rate had to be increased to 4 times. The performance of 50% water–ethylene glycol mixture was worse than water. They also reported that two-phase cooling was better at reducing local hot-spot due to high local heat flux as compared to water cooling because, unlike single-phase cooling, the flow boiling heat transfer coefficient increases with heat flux.

Wang et al. [5] evaluated drop-in performance of single-phase water, a 50% water–ethylene glycol mixture and HFC-134a two-phase cooling using a semi-empirical model for a microchannel cold plate designed to cool a EV motor inverter for 12 insulated-gate bipolar transistor (IGBT)-diode pairs. The heat flux for the IGBT and the diode were 1200 kW/m^2 and 950 kW/m^2, respectively. It was shown at equal pumping power that almost 47 °C lower IGBT temperature can be achieved with two-phase cooling as compared to 50% water–ethylene glycol mixture single-phase cooling at the same pumping power. Similarly, temperature non-uniformity in the inverter was reduced from 32 °C for water to only 3.9 °C for HFC-134a.

These studies clearly establish that pumped two-phase cooling systems have lower thermal resistance in both cold plate and condenser, provide uniform device temperature and are compact as compared to single-phase water cooled systems.

Health, safety and environmental aspects

The health, safety and environmental aspects of fluorinated fluids need attention during fluid selection. An ideal fluorinated fluid would have low toxicity and be nonflammable, and environmentally benign. These properties vary by fluid, so additional safety measures may be required for indoor usage. Fluorinated fluids with high global warming potential (GWP) can also cause long-term environmental damage as they contribute to the continuing increase in global warming.

The ASHRAE standard 34 [6] safety group classification for fluorinated fluids used for refrigerants consists of a letter (A or B), which indicates the toxicity class, followed by an Arabic numeral with or without suffix letter (1, 2L, 2, or 3), which indicates the flammability class (see Table 1). Toxicity classes A and B signify refrigerants with lower toxicity and higher toxicity, respectively, based on prescribed measures of chronic (8-hr time-weighted average value) toxicity. Class A refrigerants have no identified toxicity at concentrations ≤ 400 ppmv, while class B refrigerants have evidence of toxicity at concentrations < 400 ppmv. Flammability class 1 indicates refrigerants that do not show flame propagation in air at 60 °C and 101.3 kPa, when tested in accordance with ASTM E681. Other classes signify refrigerants with flammability; the distinction in class for flammable refrigerants depends on both the lower flammability limit and the heat of combustion. ASHRAE Standard 34 has also established the maximum refrigerant concentration limit (RCL), in air, to avoid escape-impairing effects such as asphyxiation, acute toxicity, and flammability in normally occupied, enclosed spaces.

Table 1. ASHRAE standard 34 safety group classification

	Safety group	
Higher flammability	A3	B3
Flammable	A2	B2
Lower flammability	A2L	B2L
No flame propagation	A1	B1
	Lower toxicity	Higher toxicity

This safety group classification is used in the standards (e.g., ASHRAE 15 and EN 378) and codes for determining how much refrigerant can be used in occupied areas of buildings. These standards are less restrictive for toxicity class A fluids than class B fluids. In practical terms, the standards will permit greater refrigerant charge amount and resultantly larger cooling systems for class A fluids. Similar restrictions are placed on the amount of refrigerant charge that can be used in occupied areas of buildings and equipment based on the level of flammability. Occupational safety measures can be used to minimize the risks associated with toxicity. Handheld refrigerant leak detectors can be used to pinpoint leakage. Cooling equipment- and room-level sensors can be used to monitor leaks to protect those in

proximity of the system, refrigerant conservation, equipment protection and performance, and reduction of emissions.

The Kigali Amendment of the Montreal Protocol, which came into force on January 1, 2019, requires progressive reduction of HFCs measured in CO_2-equivalence (CO_2e) available on market. Figure 1 graphically shows the phase down schedule for various regions of the world. The Regulation stipulates a stepwise decrease in HFC use of 79 per cent by 2030 compared with 2014 levels in the European Union. Other developed countries will see dramatic cut in HFC supply in 2024 and 2028. Besides the phase-down mechanisms, many governments in EU are introducing measures for reducing the consumption of high-GWP fluorinated fluid, such as GWP-weighted taxes and application-specific GWP limits. The F-gas regulation in EU has introduced the requirement of periodic leak checking of equipment containing fluorinated fluids for preventing their release into the atmosphere. The thresholds for frequency of leak checking depend on the CO_2e of the fluid quantity in the system. Therefore, fluids with higher GWP will require more frequent leak checking. These regulations and measures are encouraging the use of lower GWP alternatives. The need for stakeholders in the two-phase cooling sector is to move rapidly out of HFCs and other high GWP molecules.

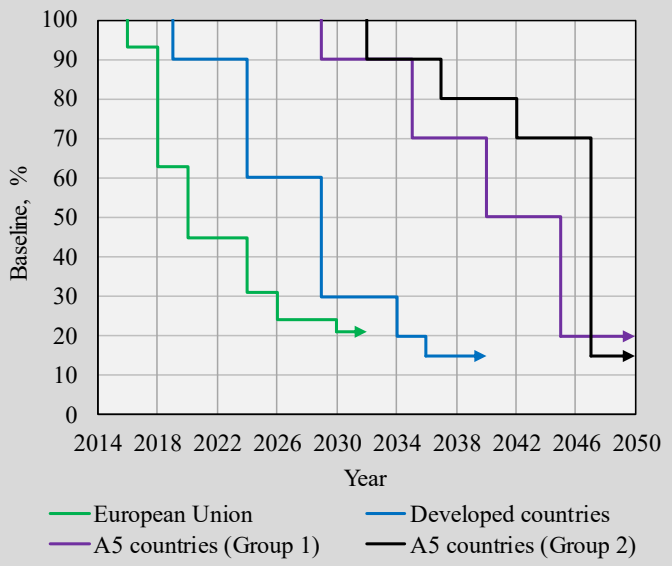

Fig. 1 HFC-phase down schedule

Heat transfer fluids for two-phase cooling

Typically, the maximum working pressure of pumped water systems is limited to 120 psi [7], and more likely in the range of 60-65 psi [8,9]. Operating pressure of systems using fluorinated fluids with normal boiling point close to room temperature will be less than 60 psi (4.13 bar) at ASHRAE W4 condition (condensing temperature of 50 ºC for facility supply-water temperature of 45 ºC). HCFO-1233zd(E), HFC-245fa and HFE-7000 are low-pressure fluid options with pressure in the working range mentioned above. The basic properties of the above heat transfer fluids are listed in Table 2. These can be alternatives for water due to their low pressure but will require new designs. Hereinafter for brevity, ASHRAE refrigerant designations will be used for HCFO-1233zd(E) and HFC-245fa, which are R-1233zd and R-245fa, respectively.

Table 2. Environmental, occupational safety and thermodynamic properties of select low-pressure heat transfer fluids.[1]

Property	R-245fa	R-1233zd	HFE-7000
Molecular formula	CF3-CH-CF3	CF3-CH=CHCI	C3F7-O-CH3
ODP[2]	0	0	0
GWP[3]	1030	1	530
OELs, ppmv	300	800	250
Flammability[4]	Nonflammable	Nonflammable	Nonflammable
Safety group[5]	B1	A1	Not classified
Boiling point at 1 atm., ºC	15.14	18.26	34.2
Pressure, bar[6]	3.44	2.93	1.74

[1] These are just some of a mosaic of properties that must be considered in selecting a suitable heat transfer fluid. Data source for thermodynamic properties: NIST REFPROP 9.1 [10]. Data source for GWP: IPCC 5th assessment report [11]. Data source for OEL, flammability and safety group of refrigerants: ASHRAE Standard 34-2019 [6]. Data source for OEL and flammability of HFE-7000: Product technical data sheet [12].
[2] CFC-11 = 1
[3] IPCC fifth assessment report (GWP CO_2 = 1)
[4] Flammability tests according to ASTM E681-04 at 21 ºC
[5] Flammability tests according to ASTM E681-09 at 60 ºC
[6] Saturated liquid at 50 ºC

Fluids that are non-ozone-depleting (ODP = 0), have low GWP, A1 safety group classification and can provide cooling performance better than water are most suitable for this application. Low-pressure fluid options such as R-245fa and HFE-7000 have a higher degree of toxicity (OEL < 400 ppm) and higher GWP as compared to R-1233zd. R-245fa is affected by the HFC-phase down, while both R-245fa and HFE-7000 may be affected by the measures such as taxation and necessity of frequent leak checking in European Union. R-1233zd is a sustainable solution as it is exempted by regulatory phase-down and even large centralized systems will not require leak checks.

Two-phase cooling in microchannels

Macro-to-microscale transition criterion for two-phase flow in channels can be defined based on the confinement number Co [13]. Confinement number is defined as

$$Co = \frac{1}{D_H}\sqrt{\frac{\sigma}{g(\rho_L - \rho_V)}} \quad (1)$$

where hydraulic diameter, D_H, of the channel is defined as

$$D_H = \frac{2WH}{W + H} \quad (2)$$

The lower boundary of macroscale flow is $Co < 0.3$, the upper boundary of symmetric microscale flow is $Co > 1$ and asymmetric microscale flow regime is in between these ranges.

Revellin and Thome [14] observed three flow regimes for R-245fa flow in microchannels, namely, isolated bubble, coalescing bubble and smooth-annular flow, in order of their appearance along the length of channel. As the channel confinement increases, these transitions occur at lower vapor qualities.

Costa-Patry et al. [15] studied two-phase pressure drop characteristics on flow boiling of R-236fa (normal boiling point: −1.4 °C) and R-245fa in rectangular channels with hydraulic diameter of 148 μm. The pressure drop increased almost linearly with the vapor quality. Karwa [1] also reported similar dependence of pressure drop on the mass flow rate for R-1233zd. R-245fa flows had a larger pressure drop than R-236fa due to this refrigerant's low vapor density. The flow-pattern based model made better predictions than other correlations based on mechanistic models.

Costa-Patry et al. [16] experimentally determined the two-phase heat transfer coefficient distribution for R-245fa along the channels of a microchannel cold plate with the exit vapor quality up to 0.6. They observed that the heat transfer coefficient first decreases along the channel, reaches a minimum value and then starts to again increase. They found that the vapor quality at the minimum heat transfer coefficient nearly coincides with the coalescing bubble flow regime to annular flow regime transition. The vapor quality at minimum heat transfer coefficient increases with heat flux and decreases with mass flux. They developed a flow pattern-based model that could capture the trends of the local heat transfer distribution, but the mean absolute error was higher than 20%. On the other hand, flow boiling correlations that are based on a weighted combination of nucleate boiling and convective heat transfer, such as the correlation by Bertsch et al. [17], predict a nearly flat or decreasing trend of heat transfer coefficient along the channel with higher error in predicting average heat transfer coefficient.

Huang et al. [18] evaluated the pressure drop and local heat transfer coefficient distribution of R-1233zd(E) in the annular flow regime. They observed that the channel pressure drop increased with the mass flux and vapor quality. Mass flux exhibited a strongly positive influence on the local heat transfer coefficient in the annular flow regime. They found that flow pattern-based model predicts the trends of the local heat transfer distribution but it underpredicts the heat transfer coefficient.

Dang et al. [19] reported the thermohydraulic performance of HFE-7000 in microchannels with hydraulic diameter of 1.33 mm and heat flux up to 300 kW/m^2. A slightly non-linear dependence of pressure drop with the vapor quality was observed and the saturation temperature drop was about 3.8 °C, which is higher than the saturation temperature for R-1233zd reported by Karwa [1].

It is important to compare the pressure drop and corresponding saturation temperature for different heat transfer fluids as the saturation temperature drop is essentially a thermal resistance in the heat transfer system. However, it is difficult to compare the pressure drop for different fluids if measurements are not made for comparable geometry, boundary and operating conditions. Similarly, a comparison of system thermal resistance for two-phase heat transfer fluids has not been reported in open literature. Huang [20] compared the pressure drop of low-pressure fluids at equal outlet vapor quality and reported similar pressure drop for R-245fa and R-1233zd. However, R-236fa has much lower pressure drop as its liquid to vapor density ratio and liquid viscosity are lowest among the three fluids.

Previous studies have not presented a drop-in performance comparison of low-pressure heat transfer fluid options for pumped two-phase cooling. The objective of this paper is to report results of drop-in performance evaluations of R-245fa, R-1233zd, HFE-7000 and water in a system with multi-microchannel copper cold plate with thermal boundary conditions comparable to that of a CPU used in HPC applications.

EXPERIMENTAL TEST SETUP AND PROCEDURE

Detailed description of the experimental setup and preparation and operating procedure was given by Karwa [1]. For continuity, a concise description is provided. A schematic of the pumped two-phase loop is shown in Fig. 2. The loop pressure was maintained by setting the fluid temperature within the expansion tank. The expansion tank was also used for regulating the amount of heat transfer fluid inside the cycle under varying operation conditions. The flow rate was adjusted using a variable speed gear pump and the mass flow rate was measured using a Coriolis mass flow meter. Inlet temperature to the cold plate was maintained using a brazed plate preheater. A water-cooled brazed plate condenser was used and the condenser water temperature was raised until a condition where loss of flow was reached due to vapor entering the pump inlet.

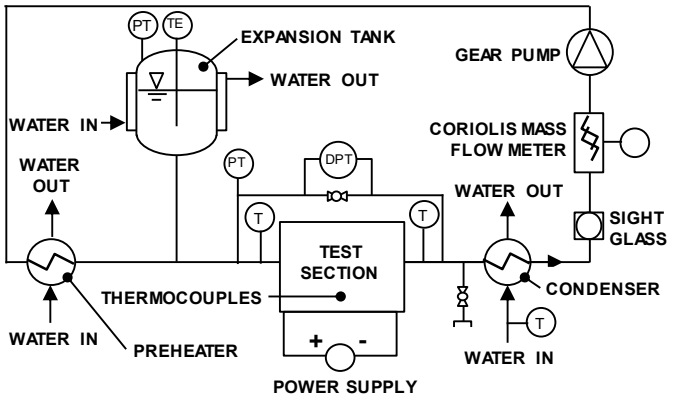

Fig. 2 Schematic of pumped two-phase cooling loop

A schematic of the test section assembly is shown in Fig. 3. The cold plate was mounted on the copper block using the thermal interface material. The cold plate is an assembly of a copper base plate, a stainless steel cover plate and a flat gasket. The copper base plate has integral fins and parallel rectangular microchannels are formed on assembly. Dimension of the formed microchannels are given in Table 3. The footprint of the finned area, A_H, is 25 × 25 sq. mm. Headers that span across all the microchannels are formed at either ends of the microchannels for fluid distribution. A circular inlet port is located at one end of the inlet header. On the other hand, the

outlet port is rectangular in shape and completely covers the outlet header to reduce the pressure drop in the port. Pressure taps were located on the inlet and outlet tubes, and thermocouples were affixed on the outer surface of the inlet and outlet tubes. Eight T-type thermocouples of 0.5 mm diameter were embedded 1.5 mm below the bottom surface of the microchannels and another two were embedded under the manifolds (see Fig. 4). Cartridge heaters embedded in the copper block were powered using a variable DC power supply. The process parameters were acquired at a rate of 6 samples per minute per channel under steady state conditions for 10 minutes and time averaged data was used in the data reduction process. The accuracy of measurement systems is given in Table 4.

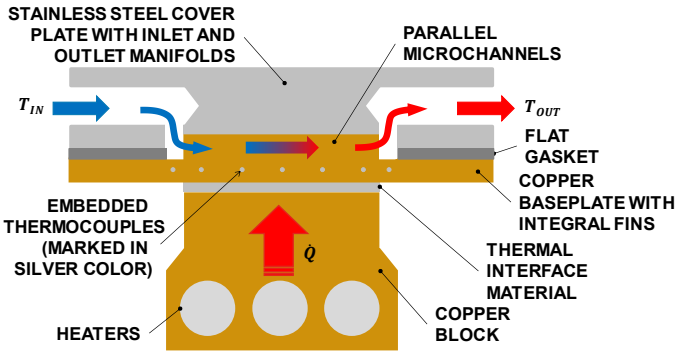

Fig. 3 Schematic of the test section

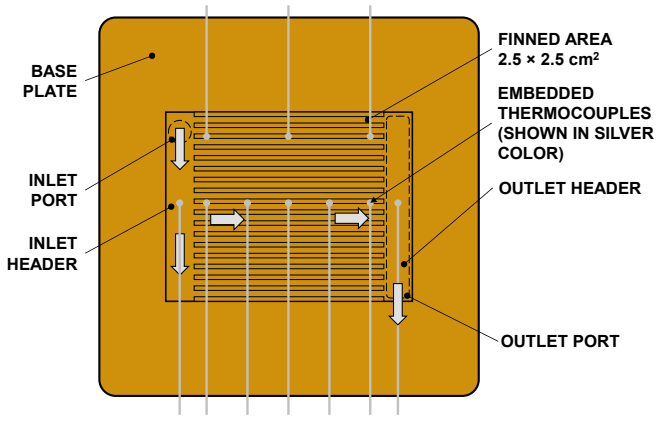

Fig. 4 Schematic of the microchannel cold plate.

Table 3. Dimensions of the microchannels

Parameter	Value
Base plate thickness, t_B, mm	3
Footprint of finned area, A_H, sq. mm	25 x 25
Microchannel length, L, mm	25
Microchannel height, H, mm	2
Channel width, W, mm	0.64
Hydraulic diameter, D_H, mm	0.97
Fin width, W_f, mm	0.64
Number of microchannels, N. -	19

In the two-phase flow experiments, the system was evacuated before the heat transfer fluid was charged into the system. Any non-condensable gases introduced into the system during charging were purged out of the system from a port at the top of the expansion tank by raising the expansion tank temperature to 50 ºC until the expansion tank pressure matched the saturation pressure at the fluid temperature. Unlike the R-1233zd and R-245fa that are supplied in cylinders, HFE-7000 is supplied in glass bottles and requires longer degassing. Additionally, since HFE-7000 has lower vapor pressure than the R-1233zd and R-245fa, its performance is penalized the most due to presence of non-condensable gases in the loop. The experiments with water were performed in an open loop with water supplied for a recirculating chiller.

Table 4. Accuracy of measurement systems

Parameter	Value
Temperature	±0.1 ºC
Absolute pressure	±2.1 kPa
Differential pressure	±0.103 kPa
Mass flow rate	±0.1% of reading
Voltage	±0.05% of reading
Current	±0.1% of reading

DATA REDUCTION AND UNCERTAINTY ANALYSIS

The heat supplied into the cold plate, Q, was calculated as

$$Q = VI \tag{3}$$

where V and I are the voltage applied across the cartridge heaters and current through the heater, respectively. Though some spreading of the heat to the inlet and outlet header area is expected, the area-averaged heat flux transferred is calculated based on the copper block area, A_H, as

$$\ddot{q} = Q/A_H \tag{4}$$

The cold plate base temperature or the junction temperature, T_J, was estimated using one-dimensional steady state heat conduction in the copper base plate:

$$T_J = T_B + \frac{\ddot{q} t_B}{2k_{CU}} \tag{5}$$

where T_B is average of the readings of the thermocouples embedded under the microchannel area, t_B is the cold plate base thickness and k_{CU} was taken as 380 W/(m·°C).

The performance of the cold plate for two-phase cooling was evaluated in the terms of thermal resistance based on the mean saturation temperature of the heat transfer fluid as

$$R_{CP} = \frac{(T_J - T_{SAT,MEAN})}{Q} \tag{6}$$

where $T_{SAT,MEAN}$ is average of the inlet and outlet saturation temperatures calculated based on the measured inlet pressure and the pressure drop across the cold plate. The saturation temperature is calculated from pressure using NIST property database REFPROP 9.1 [10].

The temperature nonuniformity is calculated as the difference between the measured maximum and minimum temperature under the microchannel area.

The performance of the for two-phase cooling system was evaluated in the terms of thermal resistance based on the condenser inlet water-supply temperature as

$$R_{SYS} = \frac{T_J - T_{C,W}}{Q} \quad (7)$$

where $T_{C,W}$ is temperature of water at the condenser inlet.

The uncertainty in thermal resistance, calculated by following the procedure in [22], was up to ±4%.

OPERATING CONDITIONS

Single-phase cooling tests with water were performed at an inlet temperature of 50 ºC, which is typical of systems designed for ASHRAE W4 class of facility inlet water-supply temperature [21]. The water flow rate was 65 kg/h and the corresponding temperature rise in the cold plate is 5.25 ºC at 400 W heat input.

Two-phase cooling tests were performed with R-1233zd and R-245fa at inlet temperature of 50 ºC and subcooling of 2±1 °C. Two-phase cooling tests with HFE-7000 were performed at two inlet saturation temperatures, 42 °C and 52 °C, and subcooling of 2±1 °C. The fluid properties and vapor pressure were obtained using NIST property database REFPROP 9.1 [8]. Asymmetric microscale flow occurs inside the microchannels as the confinement number is in the range of 0.9 to 1. The flow rate ranged from 10 to 30 kg/h. The heat input ranged from 100 and 400 W (heat flux ranged from 160 to 640 kW/m^2).

RESULTS AND DISCUSSION

The maximum junction temperature is specified by the chip manufacturer and this specification must be met by the heat sink designer. However, for the tests in the lab, it is time consuming to adjust the operating parameters to reach the specified junction temperature. Therefore, the tests were done for a fixed inlet fluid temperature and the performance for equal junction temperature was derived on the basis on thermal resistance calculations. The performance data were directly compared in the terms of average and maximum junction temperature, and temperature non-uniformity in the base plate as the results pertained to a specific cold plate.

Figure 5a shows a comparison of the junction temperature for cold plate inlet heat transfer fluid temperature of 50 ºC for water and the three two-phase cooling heat transfer fluids for a heat input of 400 W. The flow rate for all the three two-phase heat fluid was fixed at 15 kg/h. The junction temperature for two-phase cooling is lower than water cooling. The junction temperature difference between single-phase water cooling and two-phase cooling was lowest for HFE-7000 and highest for R-245fa. This meant that heat transfer coefficient is highest for R-245fa, closely followed by that of R-1233zd. However, just comparing the junction temperature for a fixed coolant temperature at the cold plate inlet is not enough as this does not tell about the total thermal budget used in the coolant loop. Therefore, a comparison of the condenser inlet water-supply temperature for the two-phase heat transfer fluids is shown in Fig. 5b. HFE-7000 requires a much lower condenser temperature than R-1233zd and R-245fa. The thermal budget used in the system is 32.2, 20.2 and 18.3 ºC for HFE-7000, R-1233zd and R-245fa, respectively.

In order to compare the performance at equal or similar junction temperatures of about 65 ºC, the performance of HFE-7000 was also evaluated at inlet temperature and subcooling of 40 ºC and 2 ºC, respectively. The junction temperature was 65.2 ºC and the condenser water temperature required for achieving a stable flow was 28 ºC, which is 19 ºC lower than that required for R-1233zd. This meant that the HFE-7000 system will operate at ASHRAE W3 condition (facility water-supply temperature of 32 °C), while R-1233zd and R-245fa are suitable for W5 condition (facility water-supply temperature of > 45 °C). Even if a larger condenser is used for HFE-7000, the maximum condenser inlet water temperature will be lower than 35 ºC as its saturation temperature at the outlet of the cold plate is ~37.5 ºC.

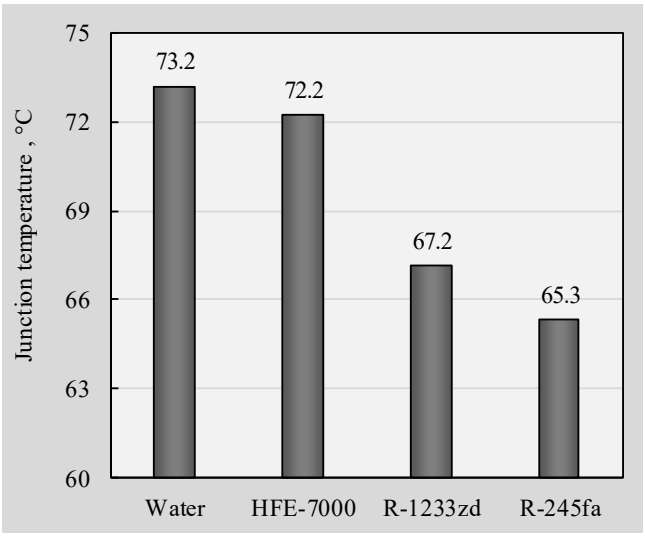

(a)

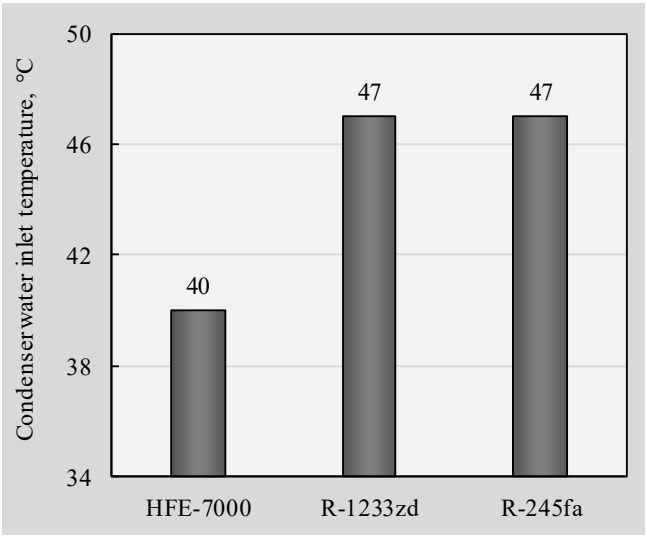

(b)

Fig. 5 Comparison of (a) junction (b) condenser inlet water-supply temperatures for a fixed cold plate inlet fluid temperature of 50 ºC

To understand the reasons for the lower performance of HFE-7000, the saturation temperature drop in the cold plate was analyzed, as saturation temperature drop is a thermal resistance in the loop. It can be seen in Fig. 6 that saturation temperature drop for R-1233zd and R-245fa for heat input of 400 W is between 1-2 ºC, which rises to 3.7 and 5.6 ºC for HFE-7000 when operated at 50 ºC and 40 ºC inlet temperature, respectively. Though not recorded in the experiment, the further saturation temperature drop will happen in the vapor line and condenser, which will increase the system thermal resistance. Indeed, to tests HFE-7000 at 400 W heat load, the ¼″ diameter tube in the vapor line used for R-1233zd and R-245fa had to be replaced with a ½″ diameter tube. The second reason for the lower performance of HFE-7000 is that the two-phase condensation heat transfer coefficient in brazed plate condensers increases with reduced pressure and vapor to liquid density ratio. HFE-7000 has lower reduced pressure than R-1233zd and R-245fa. The exit vapor quality is higher for HFE-7000 due to its lower latent heat of vaporization than R-1233zd and R-245fa, and the resulting vapor density is lower. These two factors are major contributors to the lower performance of HFE-7000 in the condenser. The third reason is that the lower vapor to liquid density and reduced pressure also contribute to the reduction in evaporation heat transfer coefficient in the microchannel cold plate.

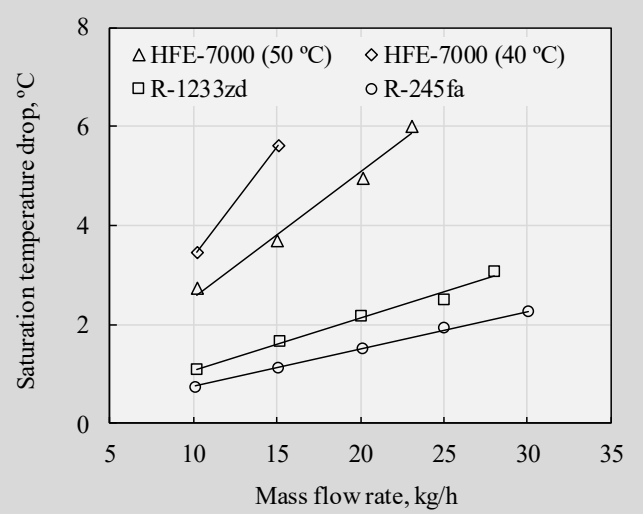

Fig. 6 Saturation temperature drop for 400 W heat input

A comparison of temperature non-uniformity across the base plate of the cold plate is shown in Fig. 7, where it is clear that HFE-7000 performance is inferior to the other low-pressure fluid options. The temperature non-uniformity for water cooling was 10.2 ºC, which is more than that of HFE-7000 cooled cold plate. It is also important to compare the maximum temperature at the base of the cold plate because a local hot spot can limit the overall performance of the cooling system. As can be seen in Fig. 8, the maximum junction temperature is almost 9 ºC higher for HFE-7000 as compared to R-1233zd, while the average temperature difference is only 5 ºC.

The thermal resistance of the cold plates at different power levels is compared in Fig. 9. Thermal resistance values for HFE-7000 and R-245fa are about 135% and 92% of R-1233zd. As thermal resistance of R-1233zd is within 10% of R-245fa, it can be near-drop in replacement of R-245fa with minor resizing of the heat exchangers. On the other hand, for HFE-7000 to match R-1233zd performance, the number of fins in the cold plate will have to be increased. However, this will further increase the pressure drop and, therefore, penalize the performance of the loop. Figure 10 compares the thermal resistance of the system. The thermal resistance of HFE-7000 increases as the saturation temperature of the heat transfer fluid at the cold plate inlet decreases. The system thermal resistance for R-1233zd is 54% of HFE-7000 at equal junction temperature of about 65 ºC. Thermal resistance of R-245fa is about 8% lower than R-1233zd.

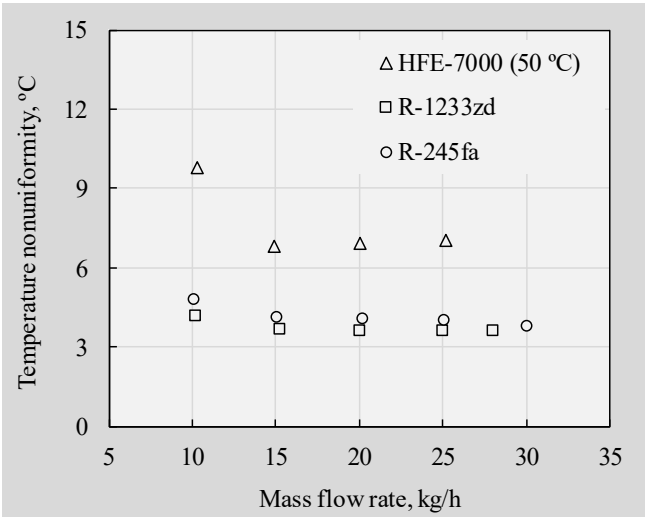

Fig. 7 Temperature nonuniformity for 400 W heat input

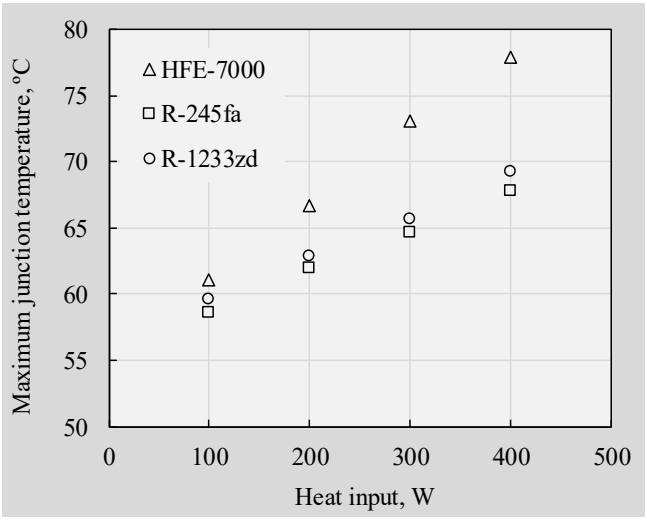

Fig. 8 Maximum junction temperature at 15 kg/h flow rate

The study demonstrates that the operating pressure of low-pressure fluid has a significant influence on the overall cooling performance and the economics of operation. With increasing chip power and number of chips per server, the pressure drop and resulting thermal resistance penalty will get severe. Therefore, use of heat transfer fluids with relatively higher pressure within the evaluated low-pressure fluids is advisable.

CONCLUSIONS

This paper reviewed the regulations and standards that impact the choice of fluorinated coolant selection. The global availability of high GWP coolants will be impacted by phase-down under the Montreal Protocol and other measures that disincentivize the use of high GWP fluids. The occupational and infrastructure safety considerations in indoor usage will favor the selection of low toxicity and non-flammable heat transfer fluid. This paper evaluated the impact of the choice of heat transfer fluids for pumped two-phase cooling of high heat dissipation server chips. Three low-pressure heat transfer fluids, namely R-1233zd, R-245fa and HFE-7000 were compared against each other and against single-phase water cooling.

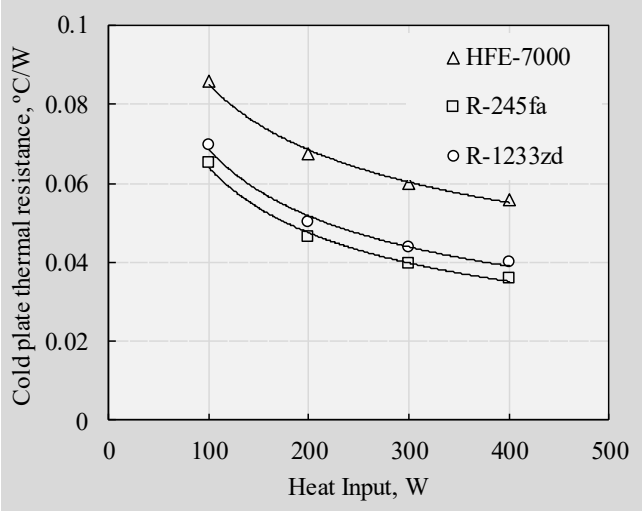

Fig. 9 Cold plate thermal resistance (heated area = 6.25 cm^2)

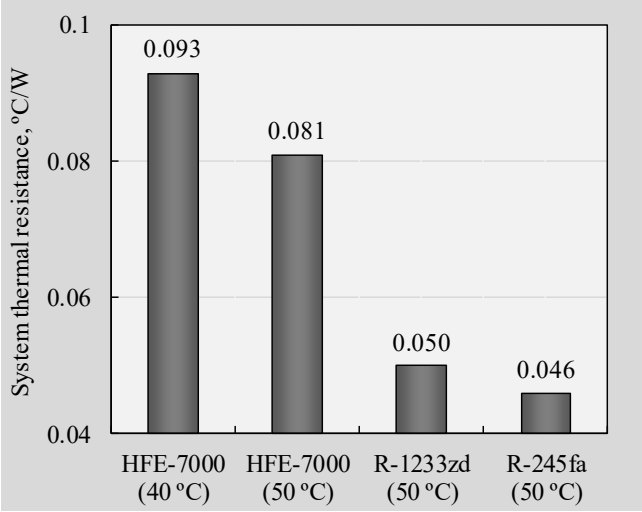

Fig. 10 System thermal resistance at 400 W heat input

The study highlights the impact of fluid saturation pressure on the system thermal resistance. With increase in saturation pressure, the heat transfer coefficient increases and additional thermal resistance due to the saturation temperature drop reduces. The drop-in loop thermal resistance for R-1233zd is 54% of HFE-7000 at equal junction temperature. Thermal resistance of R-245fa is about 8% lower than R-1233zd. Therefore, R-1233zd is a near-drop in replacement of R-245fa.

In this work, it has been demonstrated that ultra-low GWP dielectric fluid R-1233zd is a long-term option as it is more energy efficient, safer and environment-friendly than the other investigated two-phase low-pressure fluid options and water.

REFERENCES

[1] N. Karwa, "Ultra-Low Global Warming Potential Heat Transfer Fluids for Pumped Two-Phase Cooling in HPC Data Centers," in 2020 19th IEEE Intersociety Conference on Thermal and Thermomechanical Phenomena in Electronic Systems (ITherm), Orlando, FL, USA, pp. 283-290, 2020.

[2] D. Saums, "Vaporizable Dielectric Fluid Cooling of IGBT Power Semiconductors for Vehicle Powertrains," 5th IEEE Vehicle Power and Propulsion Conference, Dearborn, MI, USA, September 7–11, 2009.

[3] R. Hannemann, J. Marsala, M. Pitasi, "Pumped Liquid Multiphase Cooling," in 2004 ASME International Mechanical Engineering Congress and Exposition. Electronic and Photonic Packaging, Electrical Systems Design and Photonics, and Nanotechnology. Anaheim, CA, USA, pp. 469-473, November. 13–19, 2004.

[4] J. A Olivier, J. B. Marcinichen, A. Bruch, and J. Thome, "Green Cooling of High Performance Microprocessors: Parametric Study Between Flow Boiling and Water Cooling," ASME. J. Thermal Sci. Eng. Appl., vol. 3, no. 4, 041003, 2011.

[5] P. Wang, P, McCluskey, and A. Bar-Cohen, "Evaluation of Two-Phase Cold Plate for Cooling Electric Vehicle Power Electronics," in 2011 ASME International Mechanical Engineering Congress and Exposition. Volume 11: Nano and Micro Materials, Devices and Systems; Microsystems Integration. Denver, CO, USA, pp. 823-835, November 11–17, 2011.

[6] ANSI/ASHRAE Standard 34-2019.

[7] ASHRAE, "Water-cooled servers – common designs, components, and processes", Atlanta: ASHRAE Technical Committee (TC) 9.9, Mission Critical Facilities, Data Centers, Technology Spaces and Electronic Equipment., 2019.

[8] Lawrence Berkeley National Laboratory, "Open Specification for a Liquid Cooled Server Rack", 2018

[9] J. Gullbrand, N. Gore, J. Matteson, and E. Langer, "ACS Liquid Cooling Cold Plate Requirements Document, 2019

[10] E. W. Lemmon, M. L. Huber, and M. O. McLinden, *Reference Fluid Thermodynamic and Transport Properties – REFPROP*, Ver. 9.1. NIST, Boulder, CO, USA, 2013.

[11] IPCC WG AR – Chapter 8: Anthropogenic and Natural Radiative Forcing, February 2014.

[12] 3M™ Novec™ Engineered Fluids. http://www.3M.com.

[13] C. L. Ong and J. R. Thome, "Macro-to-microchannel transition in two-phase flow: part 1 – two-phase flow patterns and film thickness measurements," Experimental Thermal Fluid Science, vol. 35, no. 1, pp. 37-47, 2011.

[14] R. Revellin and J. R. Thome, “Experimental investigation of R-134a and R-245fa two-phase flow in microchannels for different flow conditions,” Int. J. Heat Fluid Flow, vol. 28, pp. 63-71, 2007.
[15] E. Costa-Patry, J. Olivier, B. A. Nichita, B. Michel and J. R. Thome, “Two-phase flow of refrigerants in 85 μm-wide multi-microchannels: Part I – Pressure drop,” Int. J. Heat Fluid Flow, vol. 32, pp. 451-463, 2011.
[16] E. Costa-Patry, J. Olivier, and J. R. Thome, “Heat transfer characteristics in a copper micro-evaporator and flow pattern-based prediction method for flow boiling in microchannels,” Frontiers Heat Mass Transfer, vol. 3, pp. 1-14, 2012.
[17] S. S. Bertsch, E. A. Groll, and S. V. Garimella, “A composite heat transfer correlation for saturated flow boiling in small channels,” Int. J. Heat Mass Transfer, vol. 52, no. 7–8, 2110-2118, 2009.
[18] H. Huang, N. Borhani, and J. R. Thome, “Experimental investigation on flow boiling pressure drop and heat transfer of R-1233zd(E) in a multi-microchannel evaporator,” Int. J. Heat Mass Transfer, vol. 98, pp. 596-610, 2016.
[19] C. Dang, L. Jia, Q. Peng, L. Yin and Z. Qi, “Comparative study of flow boiling heat transfer and pressure drop of HFE-7000 in continuous and segmented microchannels,” Int. J. Heat Mass Transfer, vol. 148, pp. 422-436, 2020.
[20] H. Huang, “Flow Boiling Pressure Drop and Heat Transfer of Refrigerants in Multi-microchannel Evaporators under Steady and Transient States,” PhD Thesis, EPFL, Switzerland, 2016.
[21] ASHRAE, Liquid cooling guidelines for datacom equipment centers, 2nd ed. Atlanta: ASHRAE, 2014.
[22] S. J. Kline and F. A. McClintock, “Describing uncertainties in single sample experiments,” Mechanical Engineering, vol. 75, pp. 3-8, 1953.
[23] X. Tao and C. A. I. Ferreira, “Heat transfer and frictional pressure drop during condensation in plate heat exchangers: Assessment of correlations and a new method,” Int. J. Heat Mass Transfer, vol. 135, pp. 996-1012, 2019

DISCLAIMER